Article

Inner-Sphere Electron-Transfer Reorganization Energies of Zinc Porphyrins

Xenia Amashukeli, Nadine E. Gruhn, Dennis L. Lichtenberger, Jay R. Winkler, and Harry B. Gray

J. Am. Chem. Soc., **2004**, 126 (47), 15566-15571• DOI: 10.1021/ja0351037 • Publication Date (Web): 05 November 2004

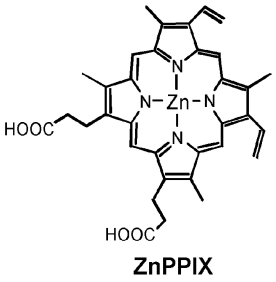

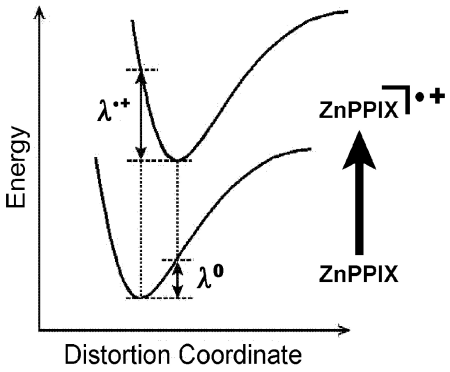

More About This Article

Additional resources and features associated with this article are available within the HTML version:

- Supporting Information
- Links to the 4 articles that cite this article, as of the time of this article download
- Access to high resolution figures
- Links to articles and content related to this article
- Copyright permission to reproduce figures and/or text from this article

View the Full Text HTML

J|A|C|S
ARTICLES
Published on Web 11/05/2004

Inner-Sphere Electron-Transfer Reorganization Energies of Zinc Porphyrins

Xenia Amashukeli,[†,§] Nadine E. Gruhn,[‡] Dennis L. Lichtenberger,*[,‡] Jay R. Winkler,[†] and Harry B. Gray*[,†]

Contribution from the Division of Chemistry and Chemical Engineering and the Beckman Institute, California Institute of Technology, Pasadena, California 91125, and Center for Gas-Phase Electron Spectroscopy, Department of Chemistry, The University of Arizona, Tucson, Arizona 85721

Received March 11, 2003; E-mail: hgcm@caltech.edu; dlichten@u.arizona.edu

Abstract: Inner-sphere electron-transfer reorganization energies of Zn(protoporphyrin IX) and Zn(octaethylporphyrin) are determined from band-shape analyses of the first ionization obtained by gas-phase valence photoelectron spectroscopy. The experimentally determined total inner-sphere reorganization energies for self-exchange (120−140 meV) indicate that structural changes upon oxidation are largely confined to the porphyrin ring, and substituents on the ring or solvent and other environmental factors make smaller contributions. Computational estimates by different models vary over a wide range and are sensitive to numerical precision factors for these low reorganization energies. Of current computational models that are widely available and practical for molecules of this size, functionals that contain a mixture of Hartree−Fock exchange and DFT exchange-correlation appear to be the most applicable.

Introduction

Hemes, the complexes of protoporphyrin IX with iron, and other metalloporphyrins are present in many enzymes and participate in a multitude of biological electron-transfer (ET) reactions.[1−3] According to semiclassical theory, the activation energies for electron-transfer reactions depend on the standard free energy change, $\Delta G°$, and the reorganization energy, λ, where $\lambda = \lambda_i + \lambda_o$, the inner- and outer-sphere contributions.[4] Ionization is itself an electron-transfer process. We have recently demonstrated that it is possible to obtain inner-sphere reorganization energies of isolated molecules from band-shape analyses of ionizations obtained by gas-phase photoelectron spectroscopy,[5−7] and Wang has used ionization band shapes to estimate the reorganization energy of the $Fe^{2+}-Fe^{3+}$ couple in iron thiolates.[8,9] As compared to other experimental methods used to analyze reorganization energies, gas-phase photoelectron spectroscopy has the advantage of allowing direct measure of λ_i without contribution from λ_o. We also have shown recently that we are able to obtain high-quality photoelectron spectra of porphyrins and metalloporphryins in the gas phase.[10,11] The combination of these developments presents the opportunity to obtain a direct energy measure of inner-sphere reorganization energies of porphryins in the gas phase, and to compare the energies with the results of high-quality calculations on isolated molecules.

While other recent computational studies have focused on the influence of different axial ligands on the reorganization energies of metal-based oxidations of heme proteins,[12,13] our focus here is the inherent reorganization energy for formation of a porphyrin-based radical cation that is often observed upon oxidation of metalloporphyrins.[2] The total inner-sphere self-exchange λ_i is the sum of the reorganization energy of the initial neutral molecule, λ^0, and the reorganization energy of the radical cation, $\lambda^{\bullet+}$. These energies are illustrated in Figure 1 in terms of a general distortion coordinate that prepares the porphyrins for electron transfer. If the distortions are sufficiently small that the transitions occur near the bottom of the potential wells, where the wells are essentially harmonic, λ^0 and $\lambda^{\bullet+}$ are similar in magnitude. Photoelectron spectroscopy directly measures the transition from state **1** to state **2** as the vertical ionization energy as shown in Figure 1, and the vibrational structure and contour of the ionization band give information on the distortion energy $\lambda^{\bullet+}$.[5] Resolved vibrational fine structure in the ionization band

[†] California Institute of Technology.
[‡] The University of Arizona.
[§] Current address: Jet Propulsion Laboratory, California Institute of Technology, 4800 Oak Grove Dr., Pasadena, CA 91109.

(1) Chapman, S. K.; Daff, S.; Munro, A. *Struct. Bonding* **1997**, *88*, 39−70.
(2) Fukuzumi, S. In *The Porphyrin Handbook*: *Electron Transfer*; Kadish, K. M., Smith, K. M., Guillard, R., Eds.; Academic Press: New York, 2000; Vol. 8, pp 115−151.
(3) *Electron Transfer in Chemistry*; Balzani, V., Ed.; Wiley-VCH Verlag: Weinheim, Germany, 2001.
(4) Marcus, R. A.; Sutin, N. *Biochim. Biophys. Acta* **1985**, *811*, 265.
(5) Amashukeli, X.; Winkler, J. R.; Gray, H. B.; Gruhn, N. E.; Lichtenberger, D. L. *J. Phys. Chem. A* **2002**, *106*, 7593−7598.
(6) Gruhn, N. E.; da Silva Filho, D. A.; Bill, T. G.; Malagoli, M.; Coropceanu, V.; Kahn, A.; Brédas, J.-L. *J. Am. Chem. Soc.* **2002**, *124*, 7918−7919.
(7) Coropceanu, V.; Malagoli, M.; da Silva Filho, D. A.; Gruhn, N. E.; Bill, T. G.; Brédas, J.-L. *Phys. Rev. Lett.* **2002**, *89*, 275503-1.
(8) Wang, W.-B.; Wang, L.-S. *J. Chem. Phys.* **2000**, *112*, 6959−6962.
(9) Yang, X.; Wang, X.-B.; Fu, Y.-J.; Wang, L.-S. *J. Phys. Chem. A* **2003**, *107*, 1703−1709.
(10) Gruhn, N. E.; Lichtenberger, D. L.; Ogura, H.; Walker, F. A. *Inorg. Chem.* **1999**, *38*, 4023−4027.
(11) Westcott, B. L.; Gruhn, N. E.; Michelsen, L. J.; Lichtenberger, D. L. *J. Am. Chem. Soc.* **2000**, *122*, 8083−8084.
(12) Sigfridsson, E.; Olsson, M. H. M.; Ryde, U. *J. Phys. Chem. B.* **2001**, *105*, 5546−5552.
(13) Rydberg, P.; Sigfridsson, E.; Ryde, U. *J. Biol. Inorg. Chem.* **2004**, *9*, 203−223.

10.1021/ja0351037 CCC: $27.50

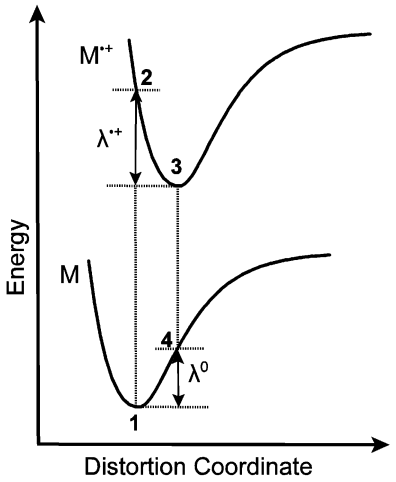

Figure 1. Potential energy surfaces for neutral and cation states that define λ^0 and $\lambda^{\bullet+}$.

Scheme 1. Structures and Abbreviations for the Molecules Studied Here

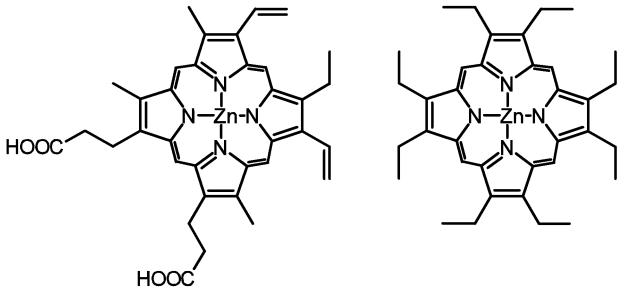

can be evaluated in terms of a distortion parameter S to give the quantum-mechanical contribution to the reorganization energy λ^{QM}. Any unresolved low-frequency modes, if present, can be treated semiclassically to give the contribution λ^{SC} after taking into account instrumental line broadening.

In agreement with Gouterman's frontier orbital model of porphyrin,[14] the first two ionizations of free base porphryins correspond to the two highest occupied π orbitals and are close in energy. If the second ionization is too close in energy to the first, it can obscure the vibrational profile associated with the lowest positive ion state. However, with the proper choice of porphyrin substituents[10] and metal,[11] these two ionizations are separated appropriately for band-shape analysis of the first ionization. Here, we measure the reorganization energies of Zn(II)(protoporphyrin IX) (Zn(ppix)) and Zn(II)(octaethylporphyrin) (Zn(oep)), the structures of which are shown in Scheme 1. These metalloporphyrins were chosen because the filled Zn 3d ionization manifold is stabilized away from the first porphryin ionizations, and the Zn substitution in addition to the functional group substitutions on the periphery of the porphyrin core provide a good separation of the first two ionizations. Specific questions to be addressed include: do the different substituents on the two porphyrins cause differences in reorganization energies; how do the reorganization energies for these metalloporphyrins compare to those for other molecules we have measured by this technique; how do the reorganization energies compare to values derived from different methods and different environments for metalloporphyrins; and how do the values measured from the gas-phase experiments compare to calculated reorganization energies for the isolated molecules?

(14) Gouterman, M. *The Porphyrins*; Dolphin, D., Ed.; Academic Press: New York, 1978.

Methods

Photoelectron Spectroscopy. Zn(ppix) was obtained from Frontier Scientific, and Zn(oep) was obtained from Aldrich. The commercial samples were used without further purification. Photoelectron spectra were recorded using a He I discharge source and an instrument equipped with a 36-cm diameter, 8-cm gap hemispherical analyzer,[15] which is described in detail elsewhere.[16] The ionization energy scale was calibrated using the difference between the $^2E_{1/2}$ ionization of methyl iodide (9.538 eV) and the $^2P_{3/2}$ ionization of argon (15.759 eV). Argon also was used as an internal calibration lock of the absolute ionization energy to control spectrometer drift throughout data collection. The instrument resolution, measured as full-width at half-maximum of the argon $^2P_{3/2}$ ionization, was 0.024 ± 0.002 eV for Zn(oep) and 0.030 ± 0.002 eV for Zn(ppix). The effective instrumental line widths at the ionization energies of interest are greater due to analyzer kinetic energy effects (0.05 ± 0.01 and 0.06 ± 0.01 eV line widths, respectively). All data were intensity corrected with an experimentally determined instrument analyzer sensitivity function, which has a linear dependence of the analyzer transmission (intensity) on the kinetic energy of the electrons within the energy range of these experiments. The displayed spectra show the ionizations produced by the He Iα photons from the source ($1s^2 \leftarrow 1s2p$, 21.218 eV). Ionizations produced by the He I β line from the source ($1s^2 \leftarrow 1s3p$, 23.085 eV), which is 3% of the intensity of the He Iα line, have been removed by spectral subtraction.

The sublimation temperatures (at $10^{-4}-10^{-5}$ Torr) were 245−275 °C (average temperature 260 °C or 533 K) for Zn(ppix) and 280−320 °C (average temperature 300 °C or 573 K) for Zn(oep). The temperatures were monitored using a "K"-type thermocouple passed through a vacuum feedthrough and attached directly to the ionization cell. During heating of the samples in vacuum, there was no evidence of decomposition products in the gas phase, and only a small amount of nonvolatile solid residue remained in the sample cell. The absorption spectrum of sublimed Zn(oep) after photoelectron data collection was identical to the absorption spectrum of the sample before data collection, indicating that no significant demetalation or other decomposition occurred during data collection.

Photoelectron Spectra Analysis. The ionization bands are represented analytically with the best fit of asymmetric Gaussian functions, which are defined by position, amplitude, and the widths at half-maximum for the high and low binding energy sides. The vertical length of each data mark in the spectra represents the experimental variance of that point. The fitting procedures are described elsewhere.[17] A minimum number of Gaussian peaks and variable parameters were used to obtain a reasonable statistical model of an ionization band intensity contour. The initial ionization peak and vibrational components were constrained to have the same symmetric widths because all are associated with similar electronic states. The Gaussians on the higher binding energy side of the bands were allowed to broaden to account for unresolved structure, electron scatter, and the rising baseline. The relative integrated peak areas are known within 5−10% confidence limits. Because of electron scatter, the major source of uncertainty was the determination of the baseline, which was assumed to be linear over the small energy range of the first ionization band in these spectra.

Reorganization Energy Analysis. The experimentally measured reorganization energy for formation of a radical cation, $\lambda^{\bullet+}$, can be

(15) Siegbahn, K.; Nordling, C.; Fahlman, A.; Nordberg, R.; Hamrin, K. *ESCA: Atomic, Molecular, and Solid State Structure Studied by Means of Electron Spectroscopy*; Almqvist & Wiksells: Uppsala, 1967.
(16) Westcott, B. L.; Gruhn, N. E.; Enemark, J. H. *J. Am. Chem. Soc.* **1998**, *120*, 3382−3386.
(17) Lichtenberger, D. L.; Copenhaver, A. S. *J. Electron Spectrosc. Relat. Phenom.* **1990**, *50*, 335−352.

considered as the sum of λ^{QM} and λ^{SC}, the reorganization energies obtained from quantum-mechanical (QM) and semiclassical (SC) band-shape analyses of photoelectron data for the first ionization of a molecule.[5] Quantum-mechanical analysis of any resolved vibrational fine structure yields distortion parameters (S), which are related to λ^{QM} according to eq 1 (h is Planck's constant and ν_k is the vibrational frequency of mode k).[18]

$$\lambda^{QM} = \sum_k h\nu_k S_k \tag{1}$$

With the assumption that the geometry changes upon ionization are small enough that a harmonic oscillator model is appropriate, the intensities of the individual symmetric Gaussian bands in the vibrational progression can be considered to follow a Poisson distribution (eq 2, where I_n is the intensity of the nth vibrational band).[18]

$$I_n = \frac{S^n}{n!}e^{-S} \tag{2}$$

For these molecules, only the first two vibrational bands are well resolved, and the values of S are extracted from the ratio of I_1 to I_0. Distortions along low-frequency modes and small frequency changes between the neutral and cation states, if present, contribute to the width of the vibrational lines in photoelectron spectra. Such band profiles were treated semiclassically (eq 3, IE is the ionization energy and D is related to the transition moment).[18]

$$G = |D|^2 \exp\frac{-(h\nu - \mathrm{IE})^2}{4k_b T\lambda^{SC}} \tag{3}$$

The Gaussian functions, $T(\nu)$, used to fit the experimental spectra[17] (eq 4, in which A is the peak height, p is the peak position, H_T is the full-width at half-maximum of function T, and α is 4 ln(2)) are convolutions of G (eq 3) and another Gaussian function, R, defined by the resolution of the instrument (eq 5).[19]

$$T(\nu) = A\exp(-\alpha)\left[\frac{(h\nu - p)}{H_T}\right]^2 \tag{4}$$

The value of H_G for the function G was obtained by iterative reconvolution of the observed line-shape function and is related to λ^{SC} according to eq 6.

$$T(\nu) = \int_0^\nu G(x)R(x-\nu)\,dx \tag{5}$$

$$\lambda^{SC} = \frac{{H_G}^2}{16\ln(2)k_b T} \tag{6}$$

Computational Details. Computational estimates of the reorganization energies of these molecules were carried out using the programs Jaguar 4.1,[20] ADF 2003,[21] Gaussian 98, and Gaussian 03.[22] The conclusions are independent of the computational package, and only the results of the calculations from the Gaussian 03 package are reported here. Unless otherwise indicated in the tables, calculations were carried out for each molecule at four points on the potential energy surfaces as illustrated in Figure 1: (1) neutral optimized geometry, charge zero, and singlet multiplicity; (2) neutral geometry, charge plus one, and doublet multiplicity; (3) radical cation geometry, charge plus one, and doublet multiplicity; and (4) radical cation geometry, charge zero, and singlet multiplicity. The energy difference between (2) and (3) is $\lambda^{\bullet+}$, and the energy difference between (4) and (1) is λ^0.[23−25] The sum of λ^0 and $\lambda^{\bullet+}$ is the total calculated reorganization energy for the self-exchange reaction. Because of the small geometry changes and energy changes in the optimizations, it was important to step through the calculations consistently in the order listed for each model and basis set. It was also necessary to achieve tight optimizations with tight SCF convergence and an ultrafine integration grid.

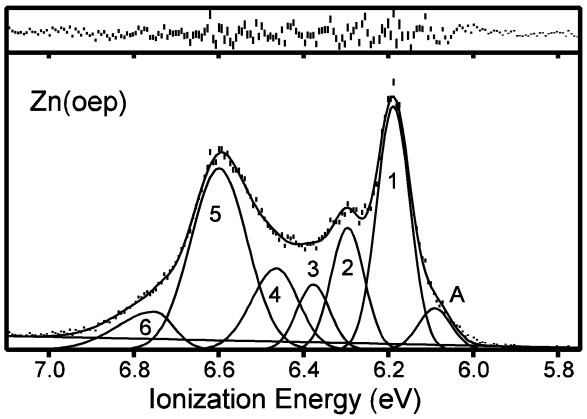

Figure 2. Photoelectron spectrum of Zn(oep) and residual of fit.

Before proceeding to Zn(oep) and Zn(ppix), a series of calculations was carried out first on Zn(porphine) to explore the dependence of the calculated reorganization energy on different computational models and basis sets. The designations of these models and basis sets in the tables are the same as in the Gaussian 03 package. All optimizations were started from geometries without strict symmetry to allow for possible dynamic Jahn−Teller distortions in the positive ions,[26] although calculations on Zn(porphine) with strict D_{4h} symmetry yielded identical energies to seven decimal places in hartrees when compared to the calculations without symmetry constraints. For the larger substituted zinc porphines, the favored conformations were selected from conformational searches carried out with the program Macromodel.[27] For Zn(oep), the favored conformation had the two ethyl groups on each pyrrole oriented with one above the plane and the other below the plane of the porphine, and mirrored between adjacent pyrroles to give the total molecule D_{2d} symmetry. For Zn(ppix), the two C(O)OH groups were oriented for maximum hydrogen bonding between them, and with the alkenes twisted about 30° out of the plane of the porphine.

Results and Discussion

Photoelectron Spectra. The He I photoelectron spectra of Zn(ppix) and Zn(oep) in the 6−7 eV region are shown in Figures 2 and 3. According to Gouterman's frontier orbital model of the electronic structure of porphyrins,[14] the two highest occupied π orbitals are close in energy, and for these molecules these

(18) Ballhausen, C. J. *Molecular Electronic Structures of Transition Metal Complexes*; McGraw-Hill: U.K., 1979; p 125.
(19) Press, W. H.; Flannery, B. P.; Teukolsky, S. A.; Vetterling, W. T. *Numerical Recipes, The Art of Scientific Computing (Fortran Version)*; Cambridge University Press: New York, 1989; p 383.
(20) *Jaguar version 4.1*; Schrodinger Inc.: Portland, OR, 2000.
(21) ADF v 2003.01, 2., SCM Inc.
(22) Frisch, M. J.; Trucks, G. W.; Schlegel, H. B.; Scuseria, G. E.; Robb, M. A.; Cheeseman, J. R.; Zakrzewski, V. G.; Montgomery, J. J. A.; Stratmann, R. E.; Burant, J. C.; Dapprich, S.; Millam, J. M.; Daniels, A. D.; Kudin, K. N.; Strain, M. C.; Farkas, O.; Tomasi, J.; Barone, V.; Cossi, M.; Cammi, R.; Mennucci, B.; Pomelli, C.; Adamo, C.; Clifford, S.; Ochterski, J.; Petersson, G. A.; Ayala, P. Y.; Cui, Q.; Morokuma, K.; Malick, D. K.; Rabuck, A. D.; Raghavachari, K.; Foresman, J. B.; Cioslowski, J.; Ortiz, J. V.; Baboul, A. G.; Stefanov, B. B.; Liu, G.; Liashenko, A.; Piskorz, P.; Komaromi, I.; Gomperts, R.; Martin, R. L.; Fox, D. J.; Keith, T.; Al-Laham, M. A.; Peng, C. Y.; Nanayakkara, A.; Challacombe, M.; Gill, P. M. W.; Johnson, B.; Chen, W.; Wong, M. W.; Andres, J. L.; Gonzalez, C.; Head-Gordon, M.; Replogle, E. S.; Pople, J. A. *Gaussian 98*, revision A.9; Gaussian, Inc.: Pittsburgh, PA, 1998.
(23) Klimkans, A.; Larsoon, S. *Chem. Phys.* **1994**, *189*, 25−31.
(24) Nelsen, S. F.; Blackstock, S. C.; Kim, Y. *J. Am. Chem. Soc.* **1987**, *109*, 677−682.
(25) Amini, A.; Harriman, A. *J. Photochem. Photobiol., C* **2003**, *4*, 155−177.
(26) Vangberg, T.; Lie, R.; Ghosh, A. *J. Am. Chem. Soc.* **2002**, *124*, 8122−8130.
(27) Macromodel 8.5, 2., Schrodinger LLC.

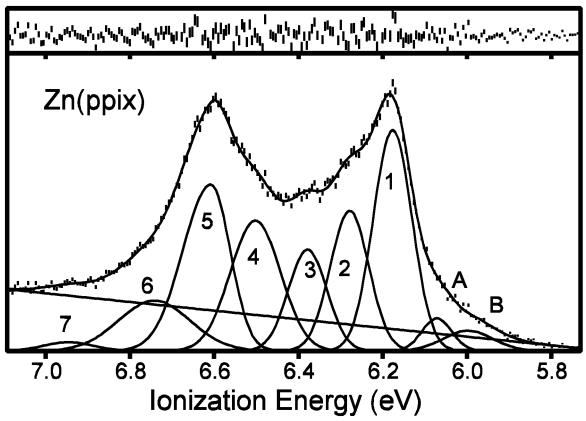

Figure 3. Photoelectron spectrum of Zn(ppix) and residual of fit.

Table 1. Analytical Gaussian Peak Representations of the First Two Zn(oep) and Zn(ppix) Ionization Profiles

ionization bands		widths (eV)		
label	energy (eV)	high	low	relative area
	Zn(oep) ($\chi^2 = 1.19$)			
1	6.19	0.092a	0.092	1
2	6.30	0.092	0.092	0.50
3	6.38	0.092	0.092	0.27
4	6.46	0.14	0.12	0.48
5	6.60	0.16	0.16	1.27
6	6.75	0.21	0.11	0.27
A	6.09	0.092	0.092	0.17
	Zn(ppix) ($\chi^2 = 0.84$)			
1	6.18	0.108[a]	0.108	1
2	6.28	0.108	0.108	0.63
3	6.38	0.108	0.108	0.46
4	6.50	0.14	0.14	0.77
5	6.61	0.16	0.11	0.92
6	6.74	0.20	0.20	0.43
7	6.95	0.14	0.14	0.05
A	6.07	0.084	0.084	0.12
B	6.00	0.14	0.14	0.12

[a] Removal of the instrument line broadening contribution to these widths at the kinetic energies of these ionizations leaves the molecular H_G values of 0.04 ± 0.01 eV for Zn(oep) and 0.05 ± 0.01 eV for Zn(ppix), which then were used to calculate λ^{SC} according to eq 6.

first two porphyrin π ionizations are cleanly separated from the ionizations above 7 eV. The parameters of the analytical representations of these ionization profiles in terms of Gaussian model peaks are given in Table 1, and the residuals of fit between the analytical representations and the data are also illustrated in the two figures.

In Figures 2 and 3, the Gaussians labeled with letters on the low binding energy side of the first main ionization model are due to hot bands. The intensities of these Gaussians are consistent with the relative intensity expected from population of excited vibrational levels in the ground state of the molecules at the temperatures at which the data were collected (245−320 °C). The vertical ionizations of the two π ionizations are associated with the two maxima on the overlapping band structure, which are modeled with the Gaussians labeled 1 and 5. The first ionizations are relatively sharp, with half-widths on the order of 0.1 eV. The second ionization envelope is broadened similar to the second ionization of pyrrole by vibronic coupling.[28] Both Zn(ppix) and Zn(oep) show a splitting of about

Table 2. Experimental Reorganization Energies for Radical Cation Formation (all λ in meV)

	$h\nu$ (eV)	S	λ^{QM}	λ^{SC}	$\lambda^{\bullet+}$
Zn(oep)	0.11 ± 0.01	0.50 ± 0.02	55 ± 3	3 ± 2	58 ± 3
Zn(ppix)	0.10 ± 0.01	0.63 ± 0.02	63 ± 3	5 ± 2	68 ± 3

0.4 eV between these two maxima, which leaves room for clear observation of the ionization intensity on the high binding energy side of the first ionization, which is due to a partially resolved vibrational progression. This structure is modeled with the Gaussians labeled 2 and 3 in the figures. The Gaussians labeled 4, 6, and 7, along with 5, model the second higher energy ionization band.

The spacing of the Gaussians 1, 2, and 3 that model the partially resolved vibrational structure on the first ionization is very similar for Zn(ppix) and Zn(oep), indicating that this structure in both spectra is due to similar vibrations. The spacing of these Gaussians is about 0.11 eV (~900 cm^{-1}), which is in the energy region expected for vibrational modes associated with the C−C and C−N bonds of the porphyrin ring. Of course, this vibrational structure is most likely the result of many vibrational modes rather than one particular mode, but the regular spacing of Gaussians can be used to represent an average of many vibrational contributions by mode averaging.[29−31]

Reorganization Energies. Several conclusions regarding the reorganization energies are visually apparent from the ionizations before proceeding to a more detailed analysis. First, the reorganization energies of these two molecules with electron transfer must be fairly similar because of the overall similarity of the vibrational profiles. As mentioned previously, the frequency of the partially resolved vibrational structure on the first ionization is very similar for Zn(ppix) and Zn(oep). Part of the broadening in the Zn(ppix) spectrum as compared to the Zn(oep) spectrum is due to the difference in instrument resolution for these two collections, but nonetheless on closer examination the greater ionization intensity on the high energy side of the first peak in the spectrum of Zn(ppix) suggests a slightly greater reorganization energy for this molecule as compared to Zn(oep). In both cases, the reorganization energy must be fairly small, because the vertical ionization is the adiabatic ionization in the partially resolved vibrational mode, and the intensity of the second vibrational component is only about one-half that of the vertical. The narrowness of the peaks that are observed indicates that the semiclassical contribution to the reorganization also is small.

The modeling of the vibrational components provides a more quantitative assessment of the reorganization energies. Values of λ^{QM}, λ^{SC}, and the relevant parameters obtained from the spectral analysis that were used to calculate these values for Zn(ppix) and Zn(oep) are given in Table 2. Because of the narrowness of the Gaussian bands, the λ^{SC} values are fairly negligible as compared to the λ^{QM} values, showing that very low-frequency modes contribute very little to the reorganization energies. The λ^{QM} value for Zn(ppix) is greater than that for Zn(oep) as expected from the visual examination, and, taken

(28) Trofimov, A. B.; Koppel, H.; Schirmer, J. *J. Chem. Phys.* **1998**, *109*, 1025−1040.
(29) Tutt, L.; Tannor, D.; Heller, E. J.; Zink, J. I. *Inorg. Chem.* **1982**, *21*, 3858−3859.
(30) Barbara, P. F.; Meyer, T. J.; Ratner, M. A. *J. Phys. Chem.* **1996**, *100*, 13148−13168.
(31) Malagoli, M.; Coropceanu, V.; da Silva Filho, D. A.; Brédas, J.-L. *J. Chem. Phys.* **2004**, *120*, 7490−7496.

together with λ^{SC}, the $\lambda^{\bullet+}$ reorganization energy for Zn(ppix) is about 10 meV greater than that for Zn(oep).

Alternative analytical models of the ionization intensity were investigated to estimate the confidence levels of the reorganization energies determined from the experimental data. Different models of the bandwidths contribute to uncertainty in the semiclassical contribution, but because this contribution is only a small portion of the total reorganization energy, it has little effect. In the quantum-mechanical portion, setting different widths and spacings of the vibrational components can yield reasonable models of the ionization profile with different intensities of the second vibrational component relative to the first. However, modeling the structure with, for example, a larger frequency gives a proportionately smaller intensity for the second vibrational component and smaller *S* value. The product of a larger frequency spacing and a smaller *S* value as in eq 1 then gives essentially the same value of λ^{QM}.

In terms of systematic errors, the perceived intensity of the first vibrational component relative to the adiabatic ionization can also be influenced by the instrumental resolution, electron scatter, the possible presence of vibronic coupling between the two energetically close ion states, or other contributions to the ionization intensity. All of these factors add intensity to the first vibrational component, and thus the reorganization energies obtained without consideration of these contributions represent upper bounds to the actual reorganization energies. We expect the error to be no more than 10%. The error may be somewhat larger for Zn(ppix) than for Zn(oep) because of the greater instrument line width during collection of the Zn(ppix) spectrum, and this may reduce the actual difference between the reorganization energies of these molecules.

The small values of $\lambda^{\bullet+}$ obtained indicate that the assumption that λ^0 is approximately the same as $\lambda^{\bullet+}$ should be reasonably valid. The self-exchange λ_i in the gas phase can then be experimentally estimated to be about 120 meV (Zn(oep)) to 140 meV (Zn(ppix)).

Computational Results. Electronic structure calculations were carried out on Zn(por) (por = unsubstituted porphyrin) before proceeding to the larger molecules to gauge the performance of different models and basis sets. On the basis of the experimental results for Zn(oep) and Zn(ppix), Zn(por) would be expected to give a similar or smaller reorganization energy, around 60 meV or less for $\lambda^{\bullet+}$ and 120 meV or less for λ_i. The results of these calculations are compared in Table 3. Calculations *a*−*d* show the basis set dependence at the Hartree−Fock level for the neutral molecules and unrestricted Hartree−Fock level for the cations. Double-ζ functions with polarization on carbon and nitrogen yield essentially the same results as triple-ζ functions with the addition of diffuse functions and polarization functions on hydrogen. The results are relatively insensitive to the basis sets on zinc, reflecting the tightness of the Zn(II) center and the small interaction of the zinc orbitals with porphyrin frontier orbitals.

All of the Hartree−Fock calculations on Zn(por) overestimate the reorganization energy by at least 50%. Initial attempts to improve these results with inclusion of correlation by limited CISD and MP2 calculations did not give better agreement. The MP2 calculations showed that attempts to improve the energies with single-point calculations at geometries obtained from other models were not internally consistent, as indicated by the λ^0 value that is much different from the $\lambda^{\bullet+}$ value in calculation *f*, and geometry optimization to less than 0.01 in coordinates was not possible. Even though tight optimization was not achieved, the results show that MP2 calculations only increased the value of the estimated reorganization energy as compared to HF calculations. In contrast to these results, MP2 calculation of reorganization energies of other organic π molecules (such as acenes to their negative ions) have been reported to decrease as compared to HF calculations.[23,32]

Table 3. Computational Estimates of Reorganization Energies (meV) of Zn(porphine)

model	basis	$\lambda^{\bullet+}$	λ^0	λ_i	opt[a]
a HF/UHF	6-31G	104	102	206	5
b	6-31G(d)	94	92	186	5
c	6-311G+(d,p)	93	91	184	6
d	TZ[b]	93	91	184	6
e CISD(G)[c]	6-31G	96	101	197	SP[d]
f MP2(FC)[f]	6-31G(d)	31	75	106	SP[e]
g		110	106	216	1000[g]
h B3LYP	6-31G(d)	68	105	173	20
i		48	48	96	5
j	TZ[b]	26	24	50	180
k		49	49	98	60[g]
l BHandHLYP	6-31G	63	62	125	2
m	6-31G(d)	63	61	124	5

[a] Maximum displacement in final optimization cycle times 10^5. [b] 6-311G(d,p) for C, N, H and CEP121 for Zn. [c] Active space of the Gouterman orbitals (two highest occupied and two lowest unoccupied orbitals). [d] Single-point calculations at the optimized neutral and cation geometries of calculation *a*. [e] Single-point calculations at the optimized neutral and cation geometries of calculation *m*. [f] Full MP2 calculations excluding core orbital electrons. [g] Cation optimization oscillating.

Density functional calculations yield more reasonable values for the reorganization energy, but only if reasonably tight geometry convergence is achieved. Unfortunately, these calculations contain an inherent instability that is difficult to predict. As shown by calculations *h*−*k*, this problem is less pronounced with larger basis sets, and possibly is related to long-range limitations in DFT[33] that lead to oscillations as one approaches tight geometry convergence. This problem was observed with ADF calculations as well. The best compromise in these calculations is the BHandHLYP functional, which contains a mixture of the Hartree−Fock exchange and DFT exchange-correlation contributions. These calculations are relatively well behaved in convergence and less basis set dependent. The BHandHLYP functional has previously been shown to be especially suitable for the description of the electronic structure and various properties of conjugated organic radical cations.[34−36]

The calculated reorganization energies for Zn(por), Zn(oep), Zn(ppix), and Zn(tpp) (tpp = tetraphenylporphyrin) by the Hartree−Fock, B3LYP, and BHandHLYP methods are compared in Table 4. The Hartree−Fock calculations always overestimate the reorganization energies, in some cases enormously so. The B3LYP calculations give reasonable estimates when tight geometry convergence is achieved, but this was not possible for the larger Zn(tpp) molecule. It is unfortunate that

(32) Larsson, S.; Klimkans, A.; Rodriguez-Monge, L.; Duskesas, G. *J. Mol. Struct. (THEOCHEM)* **1998**, *425*, 155−159.
(33) Dreuw, A.; Weisman, J. L.; Head-Gordon, M. *J. Chem. Phys.* **2003**, *119*, 2943−2946.
(34) Geskin, V. M.; Brédas, J.-L. *Int. J. Quantum Chem.* **2003**, *91*, 303−310 and references therein.
(35) Geskin, V. M.; Dkhissi, A.; Brédas, J.-L. *Int. J. Quantum Chem.* **2003**, *91*, 350−354.
(36) Geskin, V. M.; Brédas, J.-L. *ChemPhysChem* **2003**, *4*, 498−505.

Table 4. Reorganization Energies (meV) of Substituted Zn Porphines Calculated by Different Models[a]

		HF[a]	BHandHLYP[a]	B3LYP[b]	expt.
Zn(por)	$\lambda^{\bullet+}$	94	63	49	
	λ^0	92	61	49	
	λ_i	186	124	98	
Zn(oep)	$\lambda^{\bullet+}$	164	64	48	58 ± 3
	λ^0	157	63	50	
	λ_i	321	127	98	(116)[c]
Zn(ppix)	$\lambda^{\bullet+}$	269	83	63	68 ± 3
	λ^0	340	89	69	
	λ_i	609	172	132	(136)[c]
Zn(tpp)	$\lambda^{\bullet+}$	172	86	18[d]	
	λ^0	166	94	102	
	λ_i	338	180	120	

[a] 6-31G(d) basis. [b] 6-311G(d,p) basis for C, N, O, H and CEP121 basis for Zn. [c] λ_i estimated as twice $\lambda^{\bullet+}$. [d] Geometry converged to a maximum displacement of 0.0012.

more reliable estimates of reorganization energies are not available from these methods, but several conclusions are nonetheless possible. First, the assumption that $\lambda^{\bullet+}$ is similar in value to λ^0 for these molecules is apparent from those calculations that converge well. Second, the overall reorganization energies of these molecules are similar. The values for Zn(por) and Zn(oep) are nearly the same, suggesting that alkyl or related substitutions that simply increase the size of the molecule are not important. All methods agree that the reorganization energy of Zn(ppix) is larger than that of Zn(oep), suggesting that conjugation with the alkenes either in the neutral molecule or in the positive ion state could play a role.

Comparison to Other Studies. An analysis of electron-transfer kinetics in Ru−Zn−cytochrome produced an estimated upper limit of 300 meV for the inner-sphere contribution to the Zn−porphyrin self-exchange reorganization energy.[37,38] Our photoelectron spectroscopy measurements indicate that this quantity is likely to be ≤120 meV and that the outer-sphere contribution to the total reorganization energy in Ru−Zn−cytochrome is some 90 meV greater than the earlier estimate. The values of $\lambda^{\bullet+}$ for Zn(ppix) and Zn(oep) measured here are significantly lower than those measured in the same way for some polycyclic organic molecules such as 1,10-phenanthroline ($\lambda^{\bullet+} = 180$ meV) or dibenzo[*a*,*c*]anthracene ($\lambda^{\bullet+} = 158$ meV).[5] In contrast, oligoacenes, which have high electron transport mobilities in organic single crystals, have values of $\lambda^{\bullet+}$ similar to those of Zn(ppix) and Zn(oep) ($\lambda^{\bullet+} = 69.7$ meV for anthracene, $\lambda^{\bullet+} = 58.8$ meV for tetracene, $\lambda^{\bullet+} = 49.6$ meV for pentacene).[6,7] The $\lambda^{\bullet+}$ of the five-ring polycyclic dibenzo[*a*,*c*]-anthracene is more than 3 times greater than $\lambda^{\bullet+}$ of its isomer, the five-ring oligoacene pentacene. These comparisons illustrate that symmetry and electronic factors in addition to molecular size have important influences upon $\lambda^{\bullet+}$.

Conclusions

We have employed gas-phase photoelectron spectroscopy to obtain inner-sphere reorganization energies for the metalloporphyrins Zn(ppix) and Zn(oep). The values of $\lambda^{\bullet+}$ obtained from the experimental information are relatively small and only moderately influenced by the substitutions on this set of porphyrins. These small inner-sphere reorganization energies of metalloporphyrins are likely required to allow for fast ET reactions involving heme proteins.[39,40] Calculations of electron-transfer reorganization energies by methods that are currently available can have a number of difficulties, and there is not a clear path to systematically improving the results. Further theoretical investigation is called for. Photoelectron spectroscopy of the gas-phase molecules provides a direct energy measure of this reorganization that provides a valuable checkpoint for theoretical developments. Still to be considered are the effects of changing the central metal and the influence of axial ligation on the metal upon the reorganization energies of metalloporphyrins.

Acknowledgment. We thank F. Ann Walker for providing the sample of Zn(oep). This work was supported by the NSF (CHE-0078809, H.B.G., J.R.W.; CHE-0078457, D.L.L.) and the DOE (DE-FG03-95ER14574, D.L.L.).

JA0351037

(37) Winkler, J. R.; Gray, H. B. *Chem. Rev.* **1992**, *92*, 369−379.
(38) Meade, T. J.; Gray, H. B.; Winkler, J. R. *J. Am. Chem. Soc.* **1989**, *111*, 4353.
(39) Gray, H. B.; Winkler, J. R. *Annu. Rev. Biochem.* **1996**, *65*, 537−561.
(40) Gray, H. B.; Winkler, J. R. *Q. Rev. Biophys.* **2003**, *36*, 341−372.